Bioinspired Self-Healing Liquid Films for Ultradurable Electronics

Weining Miao,[†,‡,¶] Dianyu Wang,[§,¶] Zemin Liu,[∥] Jiayue Tang,[∥] Zhongpeng Zhu,[†,‡] Can Wang,[†,‡] He Liu,[∥] Li Wen,[∥] Shuang Zheng,*[,‡,⊥] Ye Tian,*[,†] and Lei Jiang[†]

[†]Laboratory of Bioinspired Smart Interfacial Science, Technical Institute of Physics and Chemistry, Chinese Academy of Sciences, Beijing 100190, People's Republic of China

[‡]University of Chinese Academy of Sciences, Beijing 100049, People's Republic of China

[§]College of Chemistry, Jilin University, Changchun 130012, People's Republic of China
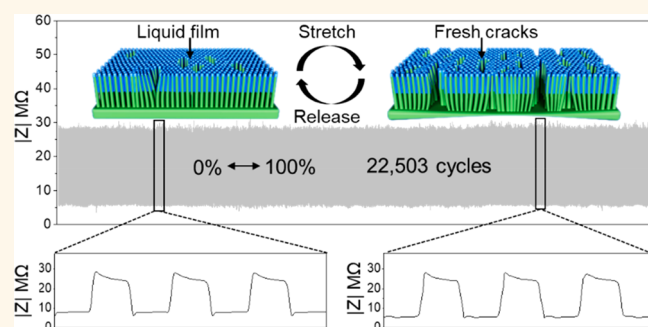
[∥]Beihang University, Beijing 100191, People's Republic of China

[⊥]Beijing National Laboratory for Molecular Sciences (BNLMS), Key Laboratory of Green Printing, Institute of Chemistry, Chinese Academy of Sciences, Beijing 100190, People's Republic of China

S *Supporting Information*

ABSTRACT: Resistive strain sensors play a crucial role in the development of flexible and stretchable electronics because of their excellent sensitivity and conformability. However, such sensors suffer from poor durability because of the low adhesion strength between the solid conductive layer and polymer and the irreparable dry friction inside the conventional solid conductive layers. Here, inspired from the structures and excellent abrasion resistance of tear films on animal corneas, we demonstrate ultradurable strain sensors based on uniform self-healing wear-free liquid films formed on biomimetic microvilli made from modified polydimethylsiloxane (PDMS). Ethanol solutions

containing ionic liquids (ILs) are added to PDMS microvilli, which are superlyophilic due to the surface chemistry and special structures. During evaporation, ILs are driven upward by Laplace pressure and join into continuous conductive films. As the sensing layer, when repeatedly stretched and released, the capillary-stabilized liquid film is lossless because of wet friction, and the cracks will recover completely after release due to the capillary-force-induced self-healing capability, allowing the strain sensors to exhibit high durability of over 22 500 loading−unloading cycles. This work presents an approach for the construction of ultradurable electronics.

KEYWORDS: *self-healing, liquid film, durability, superlyophilic, flexible sensors*

Strain sensors based on the resistive changes of conductive layers have been widely used to fabricate wearable electronics and intelligent devices because of their advantages such as high sensitivity, flexibility, and low energy consumption.[1−8] The current approaches for fabricating conductive layers are divided into two main types. The first is to fill flexible polymers with conductive materials (*e.g.*, Ag nanowires, carbon black, and metal nanoparticles), and the other is to embed or stack conductive structures (*e.g.*, aligned single-walled carbon nanotubes (SWCNTs), conductive elastomers, and metal film) onto polymer surfaces.[9−14] Strain sensors with superior performance in detecting large deformations or high sensitivities have been obtained by designing special materials or structures in previously reported researches.[15,16] However, durability is still a severe bottleneck which restricts the practical applications of these sensors. The poor durability is attributed to, first, the low adhesion strength

between the conductive layer and base and, second, the friction generated in solid conductive materials during the loading−unloading process, which is irreparable and will lead to increasing resistance and instability of the electrical signals.[17,18]

Nature offers a delicate idea to solve the above-mentioned problems. The eye surface and eyelids rub about 10 000 times per day when we blink. The excellent performance is attributed to the tear film that works as a lubricating layer and effectively avoids dry friction. Tear film is a nanostructured-microvilli-stabilized ultrathin uniform liquid film covering animal corneas, which facilitates the high durability and good abrasion resistance of the cornea. Inspired by this, we proposed
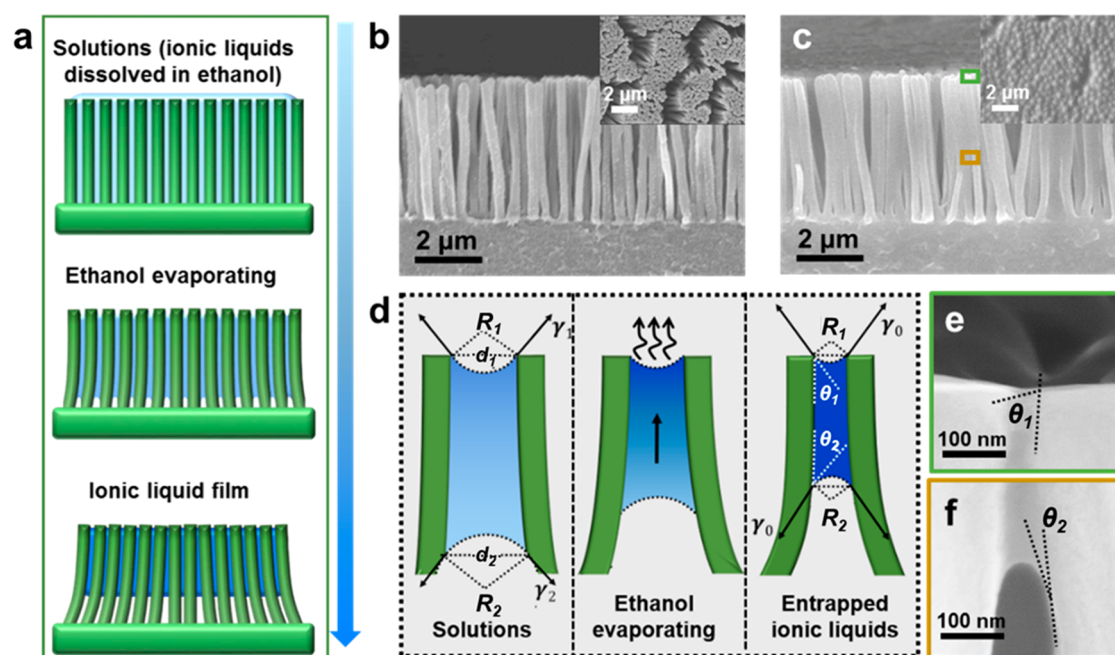
Figure 1. Fabrication of the liquid-film-based ultradurable strain sensors. (a) Formation process of the liquid film. (b, c) Cross-sectional SEM images of the microvilli without and with an ionic liquid film, respectively. Insets: Top-view SEM images. (d) Analysis of the driving force. (e, f) Meniscuses at the top and bottom of liquid film entrapped between microvilli.

biomimetic-microvilli-stabilized self-healing liquid films for fabricating ultradurable wearable strain sensors. In place of solid conductors, liquid conductive film could be an excellent candidate to improve the durability of a strain sensor because there is not any loss or abrasion when liquid films rupture and recombine and the generated cracks can heal completely by themselves after release.[19,20] Therefore, we fabricated super-lyophilic polydimethylsiloxane (PDMS) surfaces, on which an ethanol solution (containing ionic liquids (ILs)) can spread completely, resulting from interactions between the liquid and PDMS microvilli. After the ethanol evaporated, uniform-liquid-film-based strain sensors were obtained. When stretched, controlled cracks appeared on the liquid films, across which the electrical impedance magnitude (|Z|) was measured. Films at different stretch ratios showed different morphology and impedance, and the cracked liquid films were recoverable after release. As expected, our liquid-film-based strain sensors exhibited stability for more than 22 500 loading−unloading cycles at 100% strain, indicating a great improvement in durability. Moreover, the sensors could be stretched up to 200% and detect a minimum strain of 0.3%. This concept could be extended to other electronics, such as wearable humidity or chemical sensors, and provide a route to improve their durability.

RESULTS AND DISCUSSION

Fabrication of the Capillary-Stabilized Liquid Film. Elastomers based on PDMS are emerging in many fields such as wearable electronics, microfluidics, and tissue engineering because of their chemical inertness, biocompatibility, and transparency.[21−23] To fabricate a uniform ionic liquid film, the ethanol solutions of ILs generally had to spread completely on the microvilli; in other words, the substrates are super-lyophilic.[24,25] Therefore, microvilli structure was designed to improve the wettability of PDMS. First, mixtures containing PDMS prepolymers and ethoxylated polyethylenimine (PEIE,

used to enhance the stretchability) were poured onto an anodized aluminum oxide (AAO) mold (Figure S1, pore diameter ∼400 nm, center to center spacing ∼450 nm).[26] After being cured in an oven, the mold was removed to obtain the PDMS microvilli. Under the effect of van der Waal's forces (Figure S2b) between ethanol and functional groups (Figure S2a), PDMS microvilli exhibit contact angles (CAs) less than 5° for ionic liquid solutions (the light blue region in Figure S2c,d), meeting the standard of superlyophilicity. After dripping solutions onto the PDMS microvilli (Figure 1a and b), the liquid−gas interface approaches the free tips and forms a meniscus between neighboring microvilli (Figure S4) as the solvent evaporates. Surface tension subsequently drives the tips closer. An asymmetric structure appeared (Figure 1d), which is responsible for the Laplace pressure difference, as shown below:

$$F_S = 4\left(\frac{\gamma_1 S_1 \cos\theta_1}{d_1} - \frac{\gamma_2 S_2 \cos\theta_2}{d_2} \right) \tag{1}$$

where γ_1 and γ_2 are the surface tensions; θ_1 and θ_2 are the leading and trailing contact angles, respectively; d_1 and d_2 are the distances of microvilli; and S_1 and S_2 are areas of the liquid−gas interface.[27−29] It should be noted that scanning electron microscopy (SEM) reflects the real case of ILs in the sensor because the ultralow vapor pressure of ILs enables the observation of ILs in the low-pressure chamber of the SEM.[30−32] Then the Laplace pressure difference drives the liquid toward the tips, where the liquid combines to form a conductive film (Figure 1c),[33] while ILs can only become drops on PDMS without microvilli after the evaporation of the solvent (Figure S5).

The ionic liquid film can finally lose flowability and maintain stability because of the asymmetric capillary force (F_S') and the hysteresis resistance force (F_H), which are expressed as follows:
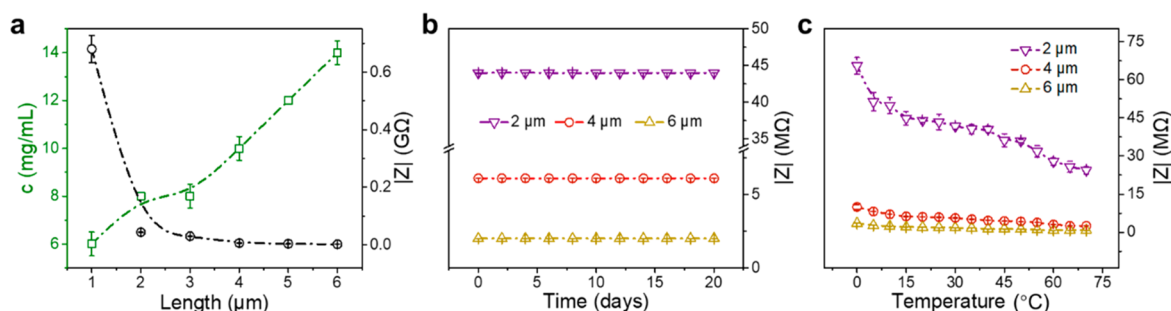
Figure 2. Characterization of the liquid films. (a) Optimal concentrations for microvilli of different lengths and the corresponding lowest impedance magnitude. (b) Impedance magnitude of the liquid-film-based sensors *versus* time, suggesting that the effect of environment is negligible. (c) Sensor impedance magnitude *versus* temperature, showing that the sensor impedance magnitude is not sensitive to temperature.
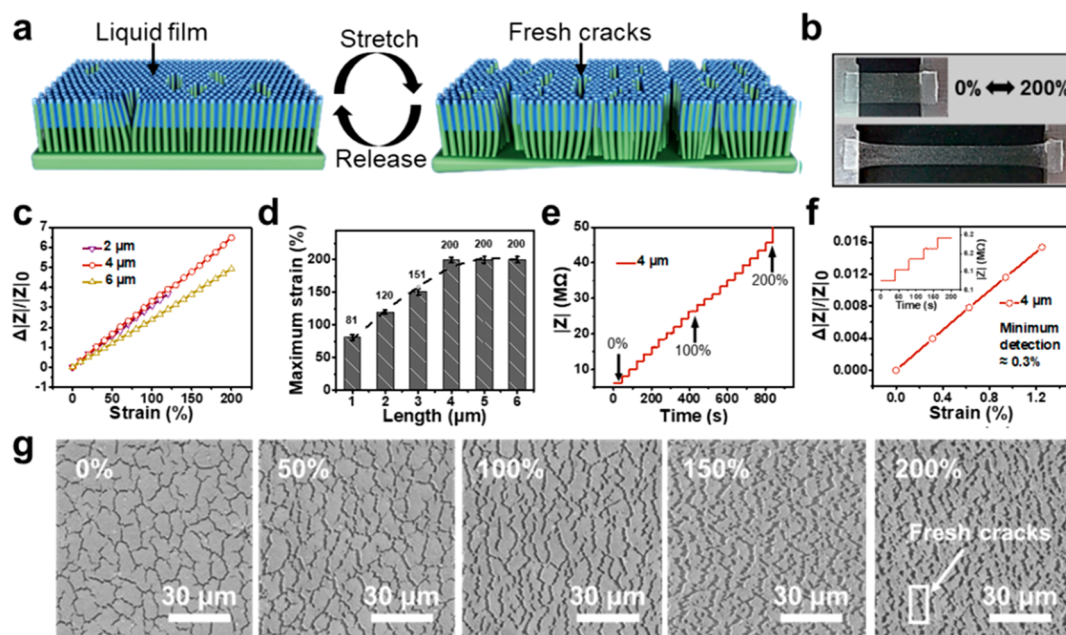

Figure 3. Mechanism and fundamental electromechanical properties of the strain sensors. (a) Illustration of the mechanism. (b) Photographs of the strain sensor in released and stretched states. (c) Relative impedance magnitude changes *versus* strain for sensors with different microvilli (length, 2, 4, 6 μm). The 4 μm length shows higher sensitivity, indicated by the slopes. (d) Maximum strain range *versus* length of the microvilli. (e) Impedance magnitude variation at a 10% step strain. (f) Relative impedance magnitude change *versus* strain ($\sim$0.3%) showing that the sensors can detect tiny deformations. The inset shows a step-strain experiment. (g) SEM images of the liquid-film-based sensors under different strain ratios.

$$F_S' = 4\left(\frac{\gamma_0 \cos\theta_1}{d_1} - \frac{\gamma_0 \cos\theta_2}{d_2}\right)S \tag{2}$$

$$S = \frac{\pi}{6}\left(R + \frac{d_1 + d_2}{2}\right)^2 - \frac{\pi}{6}R^2 \tag{3}$$

$$F_H = \gamma_0 W(\cos\theta_r - \cos\theta_a) \tag{4}$$

where γ_0 is the surface tension of the ILs; S is the cross-sectional area of ILs fixed between the microvilli; R is the radius of the microvilli; W is the length of the advancing contact line; and θ_r and θ_a are the receding and advancing contact angles, respectively.[34] After calculation (Supporting Information, Note S1), we concluded that F_S' is approximately 0.019 μN, F_H is approximately 0.041 μN, and the gravity (G) is approximately 0.0003 μN. In the balanced state, $F_S' + F_H > G$, meaning that the liquid film could not go downward. In addition, $F_H + G > F_S'$, demonstrating that the film could not

go upward. Besides, as demonstrated by the contacting experiments, the relative impedance magnitude of the sensor can be restored to the initial value after the rubber contacted and left the surface, illustrating that the liquid film on the functional surface could not be absorbed by the surface and lost (Figure S10). However, in order to keep the entrapped ionic liquids from being squeezed out under some extreme conditions in real applications, such as being compressed or kinked and so on, the sensor can be sealed by an elastomer with a low Young's modulus. After the formation of uniform IL films and casting of elastomers, the sealed air existing between microvilli and the elastomer can completely prohibit the IL from slipping out even under extreme conditions (Figure S11). In conclusion, asymmetric capillary force and the hysteresis resistance force can maintain the stability of the liquid film and satisfy the applications under common conditions.

Conductivity of the Ionic Liquid Film. For resistive strain sensors, conductive layers with stable impedance values
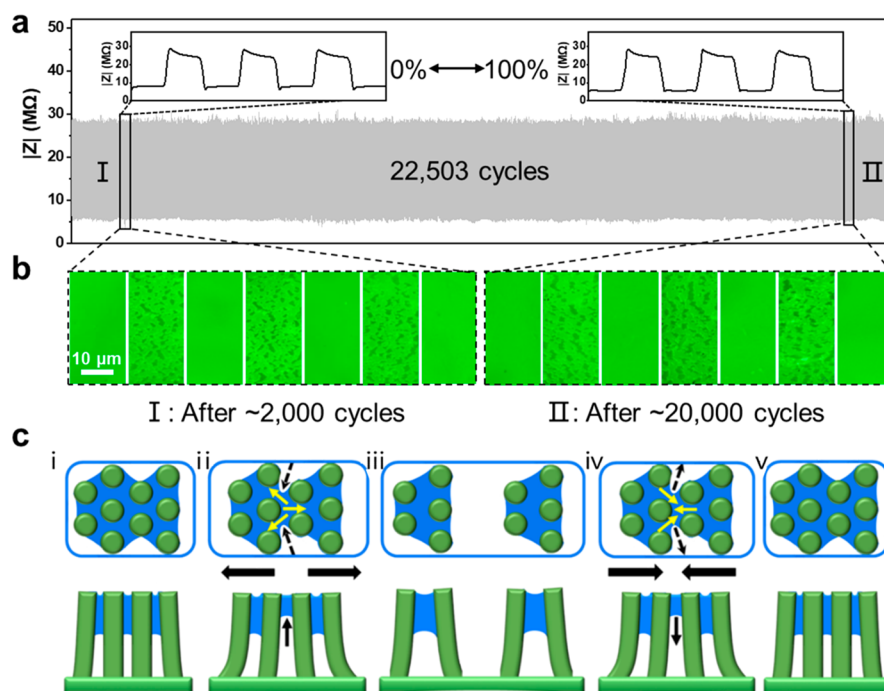
Figure 4. Durability of the strain sensors. (a) Impedance magnitude change under repeated stretch and release from 0% to 100% for over 22 500 cycles, showing excellent durability. Inset: Close-up of three cycles after 2000 cycles (I) and 20 000 cycles (II), respectively. (b) *In situ* fluorescent micrographs of the sensors in stretched and released states, respectively. (c) Schematics of the rupturing and self-healing process of the liquid film.

were strongly desired to obtain reliable electrical signals. In this work, air- and water-stable 1-butyl-3-methylimidazolium bis-(trifluoromethylsulfonyl)imide (Figure S6) was selected because of its low moisture adsorption, low surface tension, nonvolatility, and thermal stability (Table S1).[30,35] Similar to other ionic electrolytes, such ionic liquid films exhibited impedance frequency dependency (Figure S7). The impedance magnitude first sharply increases at ∼500 Hz and decreases at ∼1.2×10^4 Hz, and then remains stable between 1.2×10^4 and 1×10^6 Hz. In order to obtain impedance with high precision and excellent stability, we set a single frequency (2×10^4 Hz) to measure impedance. Nyquist plots of impedance spectra and plots of impedance magnitude of a sensor at original and stretched states are tested, respectively (Figure S8). We can obviously distinguish the increase of impedance at 2×10^4 Hz between stretched and original states. To fabricate ionic liquid films with lower impedance, we measured the impedance of sensors fabricated by ethanol solutions with different concentrations (2−16 mg/mL) and microvilli of different lengths (1−6 μm) (Figure S9). It was concluded that higher concentrations would increase the conductivity; however, there was a maximum concentration because the liquid capacity of the microvilli reservoir was limited. The optimum concentration and the corresponding impedance value are shown in Figure 2a. Surfaces with longer microvilli were endowed with greater conductivity because of the ability to accommodate more ILs. The impedance of the sensor was stable when exposed to air because the ILs are hydrophobic and chemically inert (Figure 2b). In addition, the ILs used here are not sensitive to temperature, especially for film fixed in microvilli longer than 4 μm (Figure 2c). Thus, the liquid-film-based sensor can function in a large temperature range.

Performance of the Liquid-Film-Based Strain Sensors. Figure 3a illustrates the working mechanism of the

sensor. When stretched, directional cracks appear on the capillary-stabilized continuous ionic liquid films, which results in an increase of the electric impedance. After relaxation, the cracks recovered to continuous films and the impedance was restored. Figure 3b shows the liquid-film-based strain sensor before and after stretching. Ionic liquid films on 1−6 μm microvilli were used as the strain sensors. As shown in Figure 3c, the impedance increased linearly with the stretch ratio. One important advantage of such sensors is the stretchability. Microvilli of 4 μm could detect a maximum strain of 200% (Figure 3d), much better than most of the previously reported resistive strain sensors (Table S2, Supporting Information), such as a reported nanohybrid sensor with 100% maximum strain and a graphene foam sensor with 70% maximum strain.[36,37] To evaluate the stability of the sensors, step strain experiments were conducted in which the sensors were stretched over a distance of 10% of their initial length and maintained for 40 s until the substrate ruptured (Figure 3e). When the microvilli were 4 μm, the sensors showed better sensitivity, indicated by the gauge factor (slopes of lines in Figure 3c and Figure S12). They were sensitive enough to measure a minimum strain of approximately 0.3% at an approximately 0% stretch (Figure 3f). To evaluate its response, a step strain of 22% was applied at a 33.5% stretch. The recovery time of the sensors was less than 2 s (Figure S13), faster than resistive strain sensors fabricated using solid conductors.[12] The surface structure of sensors stretched to different ratios was examined using SEM to reveal the underlying working mechanism. As shown in Figure 3g, when no tensile stress was applied, few unidirectional cracks were distributed randomly on the surfaces. After being stretched, freshly generated cracks appeared, which were vertically aligned. Further stretching led to more cracks with different widths, lengths, and densities. We constructed a
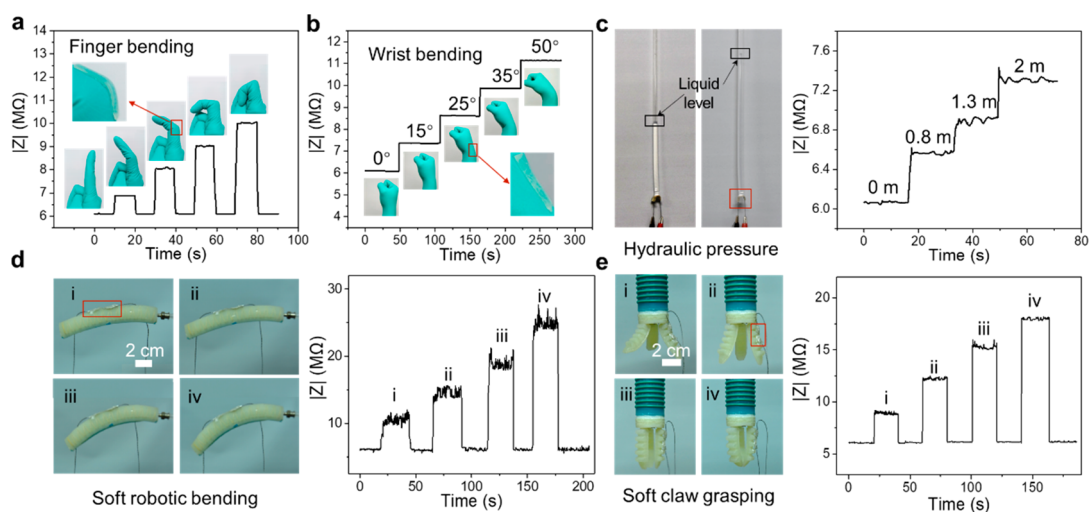
Figure 5. Applications of the liquid-film-based strain sensors. (a, b) Photographs of the strain sensor attached on a finger and a wrist, respectively, and the corresponding signals with varying degrees of bending. (c) Impedance magnitude of the strain sensor adhered to a pipe with different hydraulic levels. (d) Liquid-film-based sensor for deformation detection of a soft robot. (e) Soft mechanical hand with three claws at several states and their corresponding electronic signals. The sensors are marked by red boxes.

model to calculate the impedance change and conclude that Δ|Z| ∝ strain, which is in agreement with the experimental results (Supporting Information, Note S2).

Durability and stability are important for precise and long-term detection of deformations.[38,39] As shown in Figure 4a, our sensors exhibited stability even after being stretched for more than 22 500 cycles, during which the sensors were stretched to 100% of the original length and maintained for 5 s; then, they were released to the original position and maintained for another 5 s. To our knowledge, such sensors are more durable than most previously reported durable sensors, a graphene-based fiber sensor and a graphene-foam-based sensor both with 10 000 cycles at 50% strain (Table S2), and such improvement is attributed to the wear-free liquid conductive films.[37,40] The liquid film can recover completely after being released and even cut (Figure S15). To demonstrate this, we added trace fluorescent dye (fluorescein isothiocyanate) to the solutions during the preparation process. As shown at the bottom of Figure 4b, directional cracks formed on the liquid film after it was stretched to 100% strain and joined together after being released to the original length even after the sample was subjected to more than 20 000 strain−release cycles. Figure 4c shows how the capillary-force-stabilized liquid film ruptures and recovers. At the original position, the liquid film is distributed homogeneously among the microvilli (Figure 4c (i)). After being stretched, the distance between the PDMS microvilli increases. The ILs between the microvilli are strained and driven upward by the asymmetric capillary force, leading to temporary liquid bridges (Figure 4c (ii)). Further stretching causes greater tensile force on the liquid bridges, which finally overcomes the cohesive force and causes breakage of the liquid film. ILs fixed in the liquid bridges flow into microvilli-built reservoirs (Figure 4c (iii)). When released, the distance between microvilli decreases and the capillary tube reappears. Accelerated by the capillary force, ILs reoccupy gaps among the microvilli (Figure 4c (iv)) until the continuous film is completely recovered (Figure 4c (v)).

Applications of the Liquid-Film-Based Strain Sensors. We explore our sensor to be applied as a wearable electronic device, flexible sensor, and robotic monitor. First, after the sensor was attached to hands covered with gloves as wearable electronics, the reversible bending of knuckles (Figure 5a) and continuous bending of the wrist (Figure 5b) were distinguished. The sensors could not be directly adhered to skin until the sensor was sealed safely due to the poor biocompatibility of ILs. Second, a sensor was adhered to the bottom of a 6 mm wide pipe. As shown in Figure 5c, due to the ultraflexibility of the liquid film, our sensor could detect random and complicated deformations caused by hydraulic pressure changes. Further, a sensor was attached onto a 12 cm long pneumatically driven soft robot to monitor its deformations. As shown in Figure 5d, the relative impedance magnitude varied when the pressure in the robotic chamber increased and the robot was bent at different angles. Besides, a sensor was fixed onto a soft mechanical hand with three 5 cm long claws to monitor their activities. Different states, from splayed (i, ii in Figure 5e) to grabbed (iii, iv in Figure 5e), were clearly distinguished. These experiments reveal that our sensor can be used in many fields, including for wearable devices, flexible detectors, robot controlling, human health monitoring, and so on.

CONCLUSIONS

In summary, inspired by the tear film and cornea structure, we presented an approach for constructing ultradurable flexible sensors. By manipulating wettability and the structure of the polymer substrate, we prepared ultrathin uniform liquid conductive films, stabilized by capillary force among clustered PDMS microvilli, which are recoverable even when subjected to cyclic tensile loading. As demonstrated in the experiments, the strain sensor shows impressive durability (>22 500 cycles), because our approach overcomes the disadvantages of a traditional sensor (low adhesion strength between the solid conductors and polymer substrate and friction between solid conductors). The sensors also show a wide strain range (from 0% to 200%) and high sensitivity (minimum detection of approximately 0.3%). We believe our strain sensor will advance the development of ultradurable electronic devices and their practical applications.

EXPERIMENTAL SECTION

Fabrication of the Liquid-Film-Based Strain Sensors. PEIE (30 μL, 80% solution of ethoxylated polyethylenimine, 35−40 wt % in H_2O, average MW = 70 000, Sigma-Aldrich) and 1 g of curing agent were added to 10 g of PDMS-based elastomer (Sylgard 184, Dow Corning). The resulting mixture was mixed by hand for 5 min with a glass rod in a beaker to obtain the substrate prepolymer. A total of 0.16 mL of liquid prepolymer was dripped on the AAO mold (20 mm × 20 mm) with a uniform pore array (pore diameter ∼400 nm, center to center spacing ∼450 nm), and the prepolymer was allowed to permeate into the pores for 30 min, followed by thermal curing at 90 °C for 5 h. The substrate and AAO mold were carefully peeled from the board and soaked in HCl solution to remove the AAO mold and obtain the substrate with microvilli. The sensor was fabricated by dripping 25 μL of alcohol solution containing ionic liquids at different concentrations onto the substrate, which was allowed to remain at room temperature for 1 h to allow the alcohol to evaporate.

Structure Characterization. The morphologies of the microvilli and the surface structures were investigated using SEM (Hitachi, S-4800, Japan) at an acceleration voltage of 5.0 kV and probe current of 10 μA. Fluorescent micrographs of the surface morphology were obtained by adding fluorescein isothiocyanate to the solution, which remained in the ILs after complete evaporation of alcohol, and exciting with 470 nm blue light. An optical microscope (Vision Engineering Co., UK) connected to a CCD (charge-coupled device) camera and a desktop computer were used to obtain the micrographs.

Measurements of the Electrical Signals. The impedance signal was obtained using an LCR meter (WK6440B) at a 2.0 V alternating voltage supply. The step strain and the strain ratio of the sensor were guaranteed by attaching the sensor to a computer-controlled motion controller (Taida Machinery Equipment Co., TH16-57) using commercial double-sided adhesive tape. To study the sensor stability, the impedance variation over time was obtained for a fixed time and humidity during 20 days. The frequency-independent impedance tests were performed on an electrochemical workstation (CHI660E); testing V_{rms} was set at 0.5 V.

Wettability Characterization. The average static CAs were obtained by measuring three different positions on the same sample using a contact angle system (OCA20, Dataphysics, Germany) at ambient temperature, with the probe liquid (3 μL of water). The surface tension of the solutions was measured by removing the platinum sheet matched to the system from the solution using a highly sensitive microelectromechanical balance system (DCAT 11, Dataphysics, Germany).

ASSOCIATED CONTENT

Ⓢ Supporting Information

The Supporting Information is available free of charge on the ACS Publications website at DOI: 10.1021/acsnano.8b08911.

Notes S1 and S2, figures, and tables (PDF)

AUTHOR INFORMATION

Corresponding Authors
*E-mail (S. Zheng): zhengshuang@iccas.ac.cn.
*E-mail (Y. Tian): tianyely@iccas.ac.cn.
ORCID Ⓞ
Ye Tian: 0000-0002-1913-6333
Lei Jiang: 0000-0003-4579-728X
Author Contributions
¶W. Miao and D. Wang contributed equally to this work.
Author Contributions
S.Z., Y.T., and D.W. conceived the project. S.Z. and W.M. designed the experiment. W.M., D.W., and S.Z. fabricated the sensors. W.M. performed the testing. S.Z. and W.M. coanalyzed the results and cowrite the manuscript. W.M.

performed the calculations. Z.L. and W.M. fabricated and tested the 1D actuator and soft robotics. W.M. and Y.T. revised the papers. All authors contributed to this work. Y.T. and L.J. supervised the project.

Notes

The authors declare no competing financial interest.

REFERENCES

(1) Wan, C.; Chen, G.; Fu, Y.; Wang, M.; Matsuhisa, N.; Pan, S.; Pan, L.; Yang, H.; Wan, Q.; Zhu, L.; Chen, X. An Artificial Sensory Neuron with Tactile Perceptual Learning. *Adv. Mater.* **2018**, *30*, 1801291.

(2) Kim, Y.; Chortos, A.; Xu, W.; Liu, Y.; Oh, J. Y.; Son, D.; Kang, J.; Foudeh, A. M.; Zhu, C.; Lee, Y.; Niu, S.; Liu, J.; Pfattner, R.; Bao, Z.; Lee, T.-W. A Bioinspired Flexible Organic Artificial Afferent Nerve. *Science* **2018**, *360*, 998−1003.

(3) Chortos, A.; Liu, J.; Bao, Z. Pursuing Prosthetic Electronic Skin. *Nat. Mater.* **2016**, *15*, 937−950.

(4) Chang, J. K.; Chang, H. P.; Guo, Q.; Koo, J.; Wu, C. I.; Rogers, J. A. Biodegradable Electronic Systems in 3D, Heterogeneously Integrated Formats. *Adv. Mater.* **2018**, *30*, 1704955.

(5) Choi, S.; Lee, H.; Ghaffari, R.; Hyeon, T.; Kim, D. H. Recent Advances in Flexible and Stretchable Bio-Electronic Devices Integrated with Nanomaterials. *Adv. Mater.* **2016**, *28*, 4203−4218.

(6) Jiang, Y.; Liu, Z.; Matsuhisa, N.; Qi, D.; Leow, W. R.; Yang, H.; Yu, J.; Chen, G.; Liu, Y.; Wan, C.; Liu, Z.; Chen, X. Auxetic Mechanical Metamaterials to Enhance Sensitivity of Stretchable Strain Sensors. *Adv. Mater.* **2018**, *30*, 1706589.

(7) Jang, H.; Park, Y. J.; Chen, X.; Das, T.; Kim, M. S.; Ahn, J. H. Graphene-Based Flexible and Stretchable Electronics. *Adv. Mater.* **2016**, *28*, 4184−4202.

(8) Trung, T.-Q.; Lee, N.-E. Flexible and Stretchable Physical Sensor Integrated Platforms for Wearable Human-Activity Monitoringand Personal Healthcare. *Adv. Mater.* **2016**, *28*, 4338−4372.

(9) Kang, D.; Pikhitsa, P. V.; Choi, Y. W.; Lee, C.; Shin, S. S.; Piao, L. F.; Park, B.; Suh, K. Y.; Kim, T. I.; Choi, M. Ultrasensitive Mechanical Crack-Based Sensor Inspired by the Spider Sensory System. *Nature* **2014**, *516*, 222−226.

(10) Roh, E.; Hwang, B.-U.; Kim, D.; Kim, B.-Y.; Lee, N.-E. Stretchable, Transparent, Ultrasensitive, and Patchable Strain Sensor for Human-Machine Interfaces Comprising a Nanohybrid of Carbon Nanotubes and Conductive Elastomers. *ACS Nano* **2015**, *9*, 6252−6261.

(11) Lee, J.; Kim, S.; Lee, J.; Yang, D.; Park, B. C.; Ryu, S.; Park, I. A Stretchable Strain Sensor Based on a Metal Nanoparticle Thin Film for Human Motion Detection. *Nanoscale* **2014**, *6*, 11932−11939.

(12) Yamada, T.; Hayamizu, Y.; Yamamoto, Y.; Yomogida, Y.; Izadi-Najafabadi, A.; Futaba, D. N.; Hata, K. A Stretchable Carbon Nanotube Strain Sensor for Human-Motion Detection. *Nat. Nanotechnol.* **2011**, *6*, 296−301.

(13) Amjadi, M.; Pichitpajongkit, A.; Lee, S.; Ryu, S.; Park, I. Highly Stretchable and Sensitive Strain Sensor Based on Silver Nanowire-Elastomer Nanocomposite. *ACS Nano* **2014**, *8*, 5154−5163.

(14) Lu, N.; Lu, C.; Yang, S.; Rogers, J. Highly Sensitive Skin-Mountable Strain Gauges Based Entirely on Elastomers. *Adv. Funct. Mater.* **2012**, *22*, 4044−4050.

(15) Lipomi, D. J.; Vosgueritchian, M.; Tee, B. C. K.; Hellstrom, S. L.; Lee, J. A.; Fox, C. H.; Bao, Z. Skin-Like Pressure and Strain

Sensors Based on Transparent Elastic Films of Carbon Nanotubes. *Nat. Nanotechnol.* **2011**, *6*, 788−792.

(16) Zhao, J.; Wang, G. L.; Yang, R.; Lu, X. B.; Cheng, M.; He, C. L.; Xie, G. B.; Meng, J. L.; Shi, D. X.; Zhang, G. Y. Tunable Piezoresistivity of Nanographene Films for Strain Sensing. *ACS Nano* **2015**, *9*, 1622−1629.

(17) Lee, C. C.; Wei, P. J.; Chian, B. T.; Tsai, C. H.; Dzeng, Y. H. Predictions and Measurements of Interfacial Adhesion among Encapsulated Thin Films of Flexible Devices. *Thin Solid Films* **2015**, *584*, 154−160.

(18) Bao, Z.; Chen, X. Flexible and Stretchable Devices. *Adv. Mater.* **2016**, *28*, 4177−4179.

(19) Stogin, B. B.; Gockowski, L.; Feldstein, H.; Claure, H.; Wang, J.; Wong, T. S. Free-Standing Liquid Membranes as Unusual Particle Separators. *Sci. Adv.* **2018**, *4*, aat3276.

(20) Wong, T. S.; Kang, S. H.; Tang, S. K. Y.; Smythe, E. J.; Hatton, B. D.; Grinthal, A.; Aizenberg, J. Bioinspired Self-Repairing Slippery Surfaces with Pressure-Stable Omniphobicity. *Nature* **2011**, *477*, 443−447.

(21) Wang, Q.; Jian, M.; Wang, C.; Zhang, Y. Carbonized Silk Nanofiber Membrane for Transparent and Sensitive Electronic Skin. *Adv. Funct. Mater.* **2017**, *27*, 201605657.

(22) Au, A. K.; Huynh, W.; Horowitz, L. F.; Folch, A. 3D-Printed Microfluidics. *Angew. Chem., Int. Ed.* **2016**, *55*, 3862−3881.

(23) Kolesky, D. B.; Truby, R. L.; Gladman, A. S.; Busbee, T. A.; Homan, K. A.; Lewis, J. A. 3D Bioprinting of Vascularized, Heterogeneous Cell-Laden Tissue Constructs. *Adv. Mater.* **2014**, *26*, 3124−3130.

(24) Zheng, S.; Wang, D. Y.; Tian, Y.; Jiang, L. Superhydrophilic Coating Induced Temporary Conductivity for Low-Cost Coating and Patterning of Insulating Surfaces. *Adv. Funct. Mater.* **2016**, *26*, 9018−9025.

(25) Hou, X.; Hu, Y. H.; Grinthal, A.; Khan, M.; Aizenberg, J. Liquid-Based Gating Mechanism with Tunable Multiphase Selectivity and Antifouling Behaviour. *Nature* **2015**, *519*, 70−73.

(26) Jeong, S.-H.; Zhang, S.; Hjort, K.; Hilborn, J.; Wu, Z. Pdms-Based Elastomer Tuned Soft, Stretchable, and Sticky for Epidermal Electronics. *Adv. Mater.* **2016**, *28*, 5830−5836.

(27) Chen, H.; Zhang, P.; Zhang, L.; Liu, H.; Jiang, Y.; Zhang, D.; Han, Z.; Jiang, L. Continuous Directional Water Transport on the Peristome Surface of Nepenthes Alata. *Nature* **2016**, *532*, 85−88.

(28) Zheng, Y.; Bai, H.; Huang, Z.; Tian, X.; Nie, F.; Zhao, Y.; Zhai, J.; Jiang, L. Directional Water Collection on Wetted Spider Silk. *Nature* **2010**, *463*, 640−643.

(29) Sidorenko, A.; Krupenkin, T.; Taylor, A.; Fratzl, P.; Aizenberg, J. Reversible Switching of Hydrogel-Actuated Nanostructures into Complex Micropatterns. *Science* **2007**, *315*, 487−490.

(30) Tokuda, H.; Hayamizu, K.; Ishii, K.; Abu Bin Hasan Susan, M.; Watanabe, M. Physicochemical Properties and Structures of Room Temperature Ionic Liquids. 1. Variation of Anionic Species. *J. Phys. Chem. B* **2004**, *108*, 16593−16600.

(31) Huang, J.; Lo, Y. C.; Niu, J.; Kushima, A.; Qian, X.; Zhong, L.; Mao, S. X.; Li, J. Nanowire Liquid Pumps. *Nat. Nanotechnol.* **2013**, *8*, 277−281.

(32) Miranda, D. F.; Urata, C.; Masheder, B.; Dunderdale, G. J.; Yagihashi, M.; Hozumi, A. Physically and Chemically Stable Ionic Liquid-Infused Textured Surfaces Showing Excellent Dynamic Omniphobicity. *APL Mater.* **2014**, *2*, 056108.

(33) Wang, X. Q.; Gu, C. D.; Wang, L. Y.; Zhang, J. L.; Tu, J. P. Ionic Liquids-Infused Slippery Surfaces for Condensation and Hot Water Repellency. *Chem. Eng. J.* **2018**, *343*, 561−571.

(34) Wang, Q.; Su, B.; Liu, H.; Jiang, L. Chinese Brushes: Controllable Liquid Transfer in Ratchet Conical Hairs. *Adv. Mater.* **2014**, *26*, 4889−4894.

(35) Huddleston, J. G.; Visser, A. E.; Reichert, W. M.; Willauer, H. D.; Broker, G. A.; Rogers, R. D. Characterization and Comparison of Hydrophilic and Hydrophobic Room Temperature Ionic Liquids Incorporating the Imidazolium Cation. *Green Chem.* **2001**, *3*, 156−164.

(36) Roh, E.; Hwang, B. U.; Kim, D.; Kim, B. Y.; Lee, N. E. Stretchable, Transparent, Ultrasensitive, and Patchable Strain Sensor for Human-Machine Interfaces Comprising a Nanohybrid of Carbon Nanotubes and Conductive Elastomers. *ACS Nano* **2015**, *9*, 6252−6261.

(37) Jeong, Y.-R.; Park, H.; Jin, S. W.; Hong, S. Y.; Lee, S.-S.; Ha, J. S. Highly Stretchable and Sensitive Strain Sensors Using Fragmentized Graphene Foam. *Adv. Funct. Mater.* **2015**, *25*, 4228−4236.

(38) Wang, C.; Li, X.; Gao, E.; Jian, M.; Xia, K.; Wang, Q.; Xu, Z.; Ren, T.; Zhang, Y. Carbonized Silk Fabric for Ultrastretchable, Highly Sensitive, and Wearable Strain Sensors. *Adv. Mater.* **2016**, *28*, 6640−6648.

(39) Yan, C. Y.; Wang, J. X.; Kang, W. B.; Cui, M. Q.; Wang, X.; Foo, C. Y.; Chee, K. J.; Lee, P. S. Highly Stretchable Piezoresistive Graphene-Nanocellulose Nanopaper for Strain Sensors. *Adv. Mater.* **2014**, *26*, 2022−2027.

(40) Cheng, Y.; Wang, R.; Sun, J.; Gao, L. A Stretchable and Highly Sensitive Graphene-Based Fiber for Sensing Tensile Strain, Bending, and Torsion. *Adv. Mater.* **2015**, *27*, 7365−7371.